Synthesis and properties of soluble polyimides based on isomeric ditrifluoromethyl substituted 1,4-bis(4-aminophenoxy)benzene

Zhiming Qiu [a,b], Junhua Wang [a,b], Quanyuan Zhang [a,b], Suobo Zhang [a,*],
Mengxian Ding [a], Lianxun Gao [a]

[a] *State Key Laboratory of Polymer Physics and Chemistry, Changchun Institute of Applied Chemistry,*
Chinese Academy of Sciences, Changchun 130022, China
[b] *Graduate School of Chinese Academy of Sciences, Beijing 100049, China*

Abstract

A new fluorinated diamine monomer, [1,4-bis(4-amino-3-trifluoromethylphenoxy)benzene (**2**)], and a known isomeric analog 1,4-bis(4-amino-2-trifluoromethylphenoxy)benzene (**3**) were synthesized. A series of organosoluble polyimides **Ia−d** and **IIa** were prepared from the diamines (**2**, **3**) and dianhydrides (**a−d**) by a high-temperature one-step method. The effects of the trifluoromethyl substituents on the properties of polyimides were evaluated through the study of their soluble, thermal, optical, and gas permeability properties. Polyimides (**Ia−d**) had glass transition temperatures between 229 and 279 °C, and the temperatures at 5% weight loss ranged from 510 to 533 °C under nitrogen. These polyimides could be cast into flexible and tough membranes from DMAc solutions. The membranes had tensile strengths in the range of 137−169 MPa, tensile modulus in the range of 1.6−2.2 GPa and elongations at break from 11% to 14%. The polyimide **Ia** with trifluoromethyl groups *ortho* to the imide nitrogen exhibited enhanced gas permeability, solubility, transparency, and thermal stability compared with the isomeric polyimide **IIa** with the CF$_3$ group *meta* to the imide nitrogen. Thus, the effect of substituents in the *ortho*-positions of nitrogen on properties was greater than the effect of substituents in the *meta*-positions.
© 2006 Elsevier Ltd. All rights reserved.

1. Introduction

Aromatic polyimides are well-established high performance materials originally developed for the aerospace industry. High thermal stability combined with chemical resistance and excellent electrical and mechanical properties of polyimides make them attractive as versatile high performance materials for a variety of applications such as electrics, coatings, composite materials and membranes [1,2]. However, most polyimides also encounter processing difficulty because of their low solubility in common organic solvents and high melting or softening temperatures, which limited their some applications. To extend the utility of polyimides, much effort has been devoted to making processable polyimides based on new dianhydrides [3−10] and diamines [10−20] with the purpose of obtaining certain advantageous properties. Introducing a noncoplanar moiety into the polymer backbone, contributed either from the diamine or from the dianhydride, has been proven to be a successful approach to attain solubility without sacrificing their excellent properties. For example, 2,2′-diphenoxy-4,4′,5,5′-biphenyltetracarboxylic dianhydride [21], 2,2′-bis(4″-trimethylsilylphenyl)-4,4′,5,5′-biphenyltetracarboxylic dianhydride [22], 9,9-bis(3,5-dimethyl-4-aminophenyl)fluorene [23], and 2,2′-dinaphthylbiphenyl-4,4′-diamine [24] have been reported to effectively impart solubility without sacrificing high thermostability.

Many aromatic dianhydrides and diamines having trifluoromethyl groups can effectively impart solubility of the polyimides [25−31]. In addition, the introduction of bulky

---

* Corresponding author. Tel. +86 431 5605139.
E-mail address: sbzhang@ciac.jl.cn (S. Zhang).

trifluoromethyl moieties into the polymers would increase the free volume and decrease the dielectric constants, water absorption, and refractive indices. Polyimides based on 2,2′-bis(trifluoromethyl)benzidine [32], and 2,2′-bis(trifluoromethyl)-4,4′,5,5′-biphenyltetracarboxylic dianhydrides [33] have been reported to exhibit excellent solubility, high thermal stability and transparency in the UV–visible region. Again, a twisted noncoplanar biphenyl structure is certainly responsible for lowering the interchain interactions associated with dissolution. Furthermore, the chain rigidity of the polymer was also increased due to the substituted trifluoromethyl groups, which restricted the free rotation of the polymer backbone. Hence, the obtained polymers showed good thermal stability as well as solubility.

In the past, less investigation has been made on the effect of trifluoromethyl substituents on the properties. In this paper, we report the synthesis and characterization of isomeric polyimides derived from a new diamine monomer, 1,4-bis(4-amino-3-trifluoromethylphenoxy)benzene, and a known analog 1,4-bis(4-amino-2-trifluoromethylphenoxy)benzene. The effects of the trifluoromethyl substituents on the properties of polyimides were evaluated through the study of their thermal, optical, and gas permeability properties. We expect that the introduction of trifluoromethyl groups into *ortho*-position of the imide nitrogen hinders the rotation around the imide bonds, resulting in stiffening of the polymer chain compared to polyimides with no trifluoromethyl groups in this position, thus result in polyimides with the improved properties.

2. Experimental section

2.1. Materials

1,4-Hydroquinone, 5-chloro-2-nitrobenzotrifluoride, 2-chloro-5-nitrobenzotrifluoride, 1,4-bis(4-amino-phenoxy)benzene and isoquinoline were used as received from ACROS. 3,3′,4,4′-Biphenyltetracarboxylic dianhydride (BPDA) (ACROS) was purified by sublimation in a vacuum at 200–215 °C. 3,3′,4,4′-Benzophenonetetracarboxylic dianhydride (BTDA) (TCI) and 4,4′-oxydiphthalic dianhydride (ODPA) (TCI) was purified by recrystallization from acetic anhydride/acetic acid and dried in a vacuum oven at 120 °C for 8 h. 1,4-Bis(3,4-dicarboxyphenoxy)benzene dianhydride (HQDPA) was synthesized according to the literature [34]. Commercially obtained N,N-dimethylacetamide (DMAc), dimethyl sulfoxide (DMSO) were purified by distillation under reduced pressure from calcium hydride prior to use. m-Cresol was distilled under nitrogen before use. Other chemicals were used as received.

2.2. Measurement

The FT-IR spectra were recorded on a Bio-Rad digilab Division FTS-80 spectrometer. Thermogravimetric analysis (TGA) was performed with a Perkin–Elmer TGA-2 thermogravimetric analyzer. Experiments were carried out on approximately 4–6 mg of samples heated in flowing nitrogen or air (flow rate = 100 cm^3/min) at a heating rate of 10 °C/min.

Differential scanning calorimetry (DSC) was performed on a Perkin–Elmer DSC-7 system at a heating rate of 20 °C/min under nitrogen or air atmosphere. All melting points were determined on a Mel-Temp melting point apparatus and were uncorrected. Elemental analyses were performed on an Elemental Analyses MOD-1106. Intrinsic viscosities were determined on 0.5 g/dl concentration of polymer in DMAc using an Ubbelohde capillary viscometer at 30.0 ± 0.1 °C. ^{1}H and ^{13}C NMR spectra were measured at 300 MHz on an AV300 spectrometer with tetramethylsilane (TMS) as an internal standard. Molecular weight measurements were determined by gel permeation chromatography (GPC) using a refractive index detector. Polymer samples were dissolved in THF (30 mg/ml) and filtered through a 0.20 mm Teflon filter. All the molecular weights are measured relative to polystyrene standards. UV–visible spectra were measured with a SHIMADZU UV-2550 spectrometer in the transmittance mode. The tensile measurements were carried out on an Instron model 1122 at room temperature.

Dynamic mechanical analysis (DMTA IV, Rheometric Scientific™) was used to analyze the mechanical stability of each sample. All measurements were carried out from 50 to 250 °C by means of strain controlled mode. The strain is 0.01%. The scan rate is 3 °C/min and frequency is 1 Hz. The areas of measured samples are 1 cm × 3 cm.

The permeability was determined in the sequence of H_2, O_2, N_2, CH_4, and CO_2. They were tested at 30 °C at 1 atm. The design of permeation apparatus and detailed experimental procedure were described elsewhere [35]. In short, the gas permeability was determined from the rate of pressure increase in the permeation (downstream) side at the steady state using the following equation:

$$P = \frac{VL}{ART\Delta p}\left(\frac{\Delta p}{\Delta t}\right)$$

where P is the permeability coefficient of a membrane and its unit is barrer (1 barrer = 10^{-10} cm^3 [STP] cm cm^{-2} s^{-1} cmHg^{-1}), where V is the downstream volume, L is the membrane thickness, A is the effective area of the film, R is the universal gas constant, T is the absolute temperature, Δp is the transmembrane pressure ($=p_2 - p_1$, where p_2 and p_1 are the upstream and downstream pressures, respectively), and $\Delta p/\Delta t$ is the steady rate at which pressure increases on the downstream side. Temperature was controlled to within ± 1 °C with a thermal regulator connected to a heater in the permeation cell wall.

A wide-angle X-ray diffractometer was employed to determine the d-space of synthesized polyimides using the Cu Kα radiation wavelength. The center of the broad peak on each X-ray pattern was attributed to the average chain distance of polyimides chains. The d-spacing is calculated by substituting the scattering angles of the peak into the Bragg's equation [36], namely:

$$n\lambda = 2d \sin \theta$$

where, θ is the X-ray diffraction angle and $\lambda = 1.54$ Å.

The density ρ (g/cm^3) was determined by the flotation method in a mixture of carbon tetrachloride and xylene at 20 °C. The specific volume V_{sp} (cm^3/g) was calculated from the equation $V_{sp} = 1/\rho$.

The fractional free volume (FFV) values were calculated using experimental density values and V_w values estimated using the Bondi's group contribution method [37]. FFV was calculated using the following relationship:

$$V_f = V_{sp} - 1.3V_w$$

$$FFV = V_f/V_{sp}$$

where V_f is the free volume, V_{sp} is the specific volume, and V_w is the specific van der Waals volume, calculated using the group contribution method of Bondi, $V_0 = 1.3V_w$.

2.3. Synthesis of 1,4-bis(4-nitro-3-trifluoro-methylphenoxy)benzene (1)

1,4-Hydroquinone (4.4 g, 0.04 mol) and 5-chloro-2-nitro-benzotrifluoride (19.8 g, 0.09 mol) were first dissolved in 50 ml of dimethylsulfoxide (DMSO) in a 100 ml flask with stirring. Potassium carbonate (6.9 g, 0.05 mol) was added. After 30 min of stirring at room temperature, the mixture was heated at 100 °C for 12 h. Then, the reaction mixture was poured into 200 ml of methanol/water (volume ratio: 10:1), and the precipitated yellow solid was collected by filtration. The yield of product was 18.69 g (95.7%). The crude product was recrystallized from DMF/methanol to give fine, yellow crystals. Mp: 150.0–150.5 °C. ^{1}H NMR (CDCl$_3$, δ ppm): 7.24 (s, 6H, Ar–H), 7.45–7.46 (d, 4H, Ar–H), 8.02–8.05 (d, 4H, Ar–H). Anal. Calcd for C$_{20}$H$_{10}$F$_6$N$_2$O$_6$ (488.29): C, 49.19; N, 5.74; H, 2.06. Found: C, 49.32; N, 5.68; H, 2.01.

2.4. Synthesis of 1,4-bis(4-amino-3-trifluoro-methylphenoxy)benzene (2)

A mixture of the dinitro compound **1** (19.5 g, 0.04 mol), 10% Pd/C (0.150 g), ethanol (240 ml), and hydrazine monohydrate (20 ml) was heated at reflux temperature for about 6 h. The reaction solution was filtered when hot to remove Pd/C, and the filtrate was dried by rotary evaporation. The crude product was recrystallized from ethanol to afford 15.11 g (82%) of yellow powders. Mp: 76.0–76.5 °C. ^{1}H NMR (CDCl$_3$, δ ppm): 4.04 (br, 4H, NH$_2$), 6.72–6.74 (d, 2H, Ar–H), 6.89 (s, 4H, Ar–H), 6.99–7.02 (dd, 2H, Ar–H), 7.12–7.13 (d, 2H, Ar–H). ^{13}C NMR (CDCl$_3$): δ 153.8, 148.9, 141.0, 132.2, 126.6, 124.8, 123.0, 119.6, 119.2, 117.8, 115.6, 115.2, 114.8, 114.4 ppm. Anal. Calcd for C$_{20}$H$_{14}$F$_6$N$_2$O$_2$ (428.33): C, 56.08; N, 6.54; H, 3.29. Found: C, 56.44; N, 6.49; H, 3.26.

2.5. Synthesis of 1,4-bis(4-amino-2-trifluoro-methylphenoxy)benzene (3)

1,4-Bis(4-amino-2-trifluoromethylphenoxy)benzene was synthesized according to the literature [30], mp: 133.6–134.2 °C, yield 76%.

2.6. Polymer synthesis

Polyimide **Ia** is given as an example. Diamine **2** (0.4283 g, 1.0 mmol) and HQDPA (0.4023 g, 1.0 mmol) were first dissolved in 10.0 ml of *m*-cresol in a 50 ml three-necked round bottom flask. After the mixture was stirred at room temperature for 30 min, isoquinoline (ca. 5 drops) was added, and further stirring was conducted. Then the mixture was heated at 180 °C for 6 h. Water formed during the imidization was continuously removed with a stream of nitrogen. At the end of the reaction, the mixture was cooled and precipitated into 50 ml ethanol. The polymer was separated by filtration and washed with ethanol for several times and dried in a vacuum oven at 80 °C for 24 h.

2.7. Spectroscopic data of the polymers

2.7.1. Polyimide Ia
This polyimide was synthesized from 1,4-bis(4-amino-3-trifluoromethylphenoxy)benzene and HQDPA. The yield was 96%. ^{1}H NMR (CDCl$_3$, δ ppm): 7.22–7.24 (8H, d, Ar), 7.33–7.35 (4H, m, Ar), 7.43–7.52 (6H, m, Ar), 7.96–7.99 (2H, d, Ar). FT-IR (KBr pellet): 1784 (asym C=O str), 1732 (sym C=O str), 1380 (C–N str), 749 cm^{-1} (imide ring deformation). Anal. Calcd for C$_{42}$H$_{20}$F$_6$N$_2$O$_8$ (794.61): C, 63.48; N, 3.53; H, 2.54. Found: C, 61.32; N, 3.62; H, 2.61.
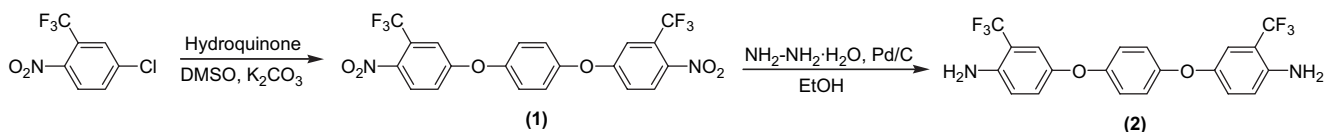
2.7.2. Polyimide Ib
This polyimide was synthesized from 1,4-bis(4-amino-3-trifluoromethylphenoxy)benzene and ODPA. The yield was 98%. ^{1}H NMR (CDCl$_3$, δ ppm): 7.23 (4H, s, Ar), 7.29–7.35 (4H, m, Ar), 7.48 (2H, s, Ar), 7.53–7.56 (2H, d, Ar), 7.62 (2H, s, Ar), 8.05–8.08 (2H, d, Ar). FT-IR (KBr pellet): 1787 (asym C=O str), 1735 (sym C=O str), 1381 (C–N str), 751 cm^{-1} (imide ring deformation). Anal. Calcd for C$_{36}$H$_{16}$F$_6$N$_2$O$_7$ (702.51): C, 61.55; N, 3.99; H, 2.30. Found: C, 60.98; N, 4.03; H, 2.34.

2.7.3. Polyimide Ic
This polyimide was synthesized from 1,4-bis(4-amino-3-trifluoromethylphenoxy)benzene and BPDA. The yield was 98%. ^{1}H NMR (CDCl$_3$, δ ppm): 7.24 (4H, s, Ar), 7.30–7.41 (4H, m, Ar), 7.50 (2H, s, Ar), 8.15 (4H, s, Ar), 8.29 (2H, s, Ar). FT-IR (KBr pellet): 1782 (asym C=O str), 1730 (sym C=O str), 1378 (C–N str), 743 cm^{-1} (imide ring deformation). Anal. Calcd for C$_{36}$H$_{16}$F$_6$N$_2$O$_6$ (686.51): C, 62.98; N, 4.08; H, 2.35. Found: C, 59.79; N, 4.23; H, 2.40.

2.7.4. Polyimide Id
This polyimide was synthesized from 1,4-bis(4-amino-3-trifluoromethylphenoxy)benzene and BTPA. The yield was 94%. ^{1}H NMR (CDCl$_3$, δ ppm): 7.24 (4H, s, Ar), 7.30–7.39 (4H, m, Ar), 7.49 (2H, s, Ar), 8.18–8.20 (2H, d, Ar), 8.31–8.35 (4H, m, Ar). FT-IR (KBr pellet): 1785 (asym C=O str), 1735 (sym C=O str), 1380 (C–N str), 750 cm^{-1} (imide ring deformation). Anal. Calcd for C$_{37}$H$_{16}$F$_6$N$_2$O$_6$ (714.52): C, 62.19; N, 3.92; H, 2.26. Found: C, 60.10; N, 4.12; H, 2.34.

Scheme 1. Synthesis of 1,4-bis(4-amino-3-trifluoromethylphenoxy)benzene.

2.7.5. Polyimide IIa

This polyimide was synthesized from 1,4-bis(4-amino-2-trifluoromethylphenoxy)benzene and HQDPA in the same method as above. The yield was 97%. ^{1}H NMR (DMSO-d_6, δ ppm): 7.22–7.34 (10H, m, Ar), 7.47–7.52 (4H, m, Ar), 7.71–7.74 (2H, d, Ar), 7.93 (2H, s, Ar), 7.99–8.01 (2H, d, Ar). FT-IR (KBr pellet): 1779 (asym C=O str), 1725 (sym C=O str), 1379 (C–N str), 744 cm^{-1} (imide ring deformation). Anal. Calcd for $C_{42}H_{20}F_6N_2O_8$ (794.61): C, 63.48; N, 3.53; H, 2.54. Found: C, 60.45; N, 3.60; H, 2.64.

2.7.6. Polyimide IIIa

This polyimide was synthesized by the two-step method: HQDPA was added to a stirred solution of 1,4-bis(4-aminophenoxy)benzene in DMAc (solid content 10% w/v) under N_2 at ambient temperature for 12 h. The poly(amic acid) solution was then cast onto a glass plate. The poly(amic acid) was converted into polyimide by successive heating in a vacuum at 80 °C for 1 h, 200 °C for 1 h, and then at 250 °C for 3 h. The yield was 90%. FT-IR (KBr pellet): 1776 (asym C=O str), 1715 (sym C=O str), 1372 (C–N str), 742 cm^{-1} (imide ring deformation). Anal. Calcd for $C_{40}H_{22}N_2O_8$ (658.61): C, 72.95; N, 4.25; H, 3.37. Found: C, 73.13; N, 4.10; H, 3.29.

2.8. Preparation of dense membranes

N,N-Dimethylacetamide (DMAc) solution of the polymers (5–7 wt%) was prepared at room temperature. The DMAc solution was filtered and cast onto a glass plate. The solvent was evaporated at 60 °C for 5 h. The membranes were then placed in a vacuum oven at 60 °C for 2 h and then 200 °C for 10 h to remove the residue solvent.

3. Results and discussion

3.1. Monomer synthesis

The synthetic route for diamine (2) is outlined in Scheme 1. The diphenolate anion, which was formed by reacting 1,4-hydroquinone with potassium carbonate, underwent aromatic nucleophilic displacement reaction with 5-chloro-2-nitrobenzotrifluoride to yield dinitro (1), 1,4-bis(4-nitro-3-trifluoromethylphenoxy)benzene. Diamine (2), 1,4-bis(4-amino-3-trifluoromethylphenoxy)benzene, was obtained in high yield by reduction of the dinitro (1) with hydrazine hydrate and Pd/C catalyst in refluxing ethanol. The dinitro (1) and diamine (2) were characterized by elemental analysis, IR, ^{1}H and ^{13}C NMR. Fig. 1 shows the IR spectra of the dinitro intermediate and the diamine. The nitro group of dinitro (1) gives two strong absorptions at 1525 and 1338 cm^{-1} (NO$_2$ asymmetric and symmetric stretching, respectively). After reduction, the characteristic absorptions of the nitro group disappeared, and the pair of N–H stretching bands of the amino group was shown in the region 3300–3500 cm^{-1}. ^{1}H NMR spectrum of diamine (2) (Fig. 2) confirms that the nitro groups have been converted into amino groups by the high field shift of the aromatic protons and by the signal at δ 4.04 ppm corresponding to the amino protons. The ^{13}C NMR spectrum of diamine monomer (2) shows two clear quartets because of the heteronuclear ^{13}C–^{19}F coupling.

3.2. Synthesis and characterization of polymers

The fluorinated diamine 2 was reacted with different dianhydride a–d with a conventional one-step procedure to give the polyimides Ia–d as displayed in Scheme 2. Polyimides are commonly synthesized via low temperature polycondensation of diamines and dianhydrides in aprotic dipolar solvents, e.g., DMAc and NMP. In this study, the polycondensation of the diamine monomer 2 and various dianhydride did not give high molecular weight polyimides under this condition because of the steric hindrance of the CF$_3$ groups. Therefore, a one-step method at a high temperature using m-cresol as the solvent was adopted in this study. For comparison study, polyimides IIa and IIIa were also synthesized from dianhydride HQDPA and known analog 1,4-bis(4-amino-2-trifluoromethylphenoxy)-benzene and nonfluorinated 1,4-bis(4-aminophenoxy)benzene, respectively. Polyimide IIIa is not soluble in m-cresol, so it
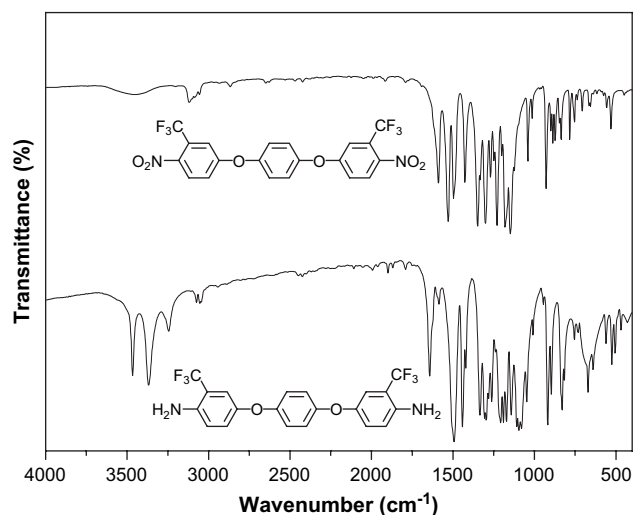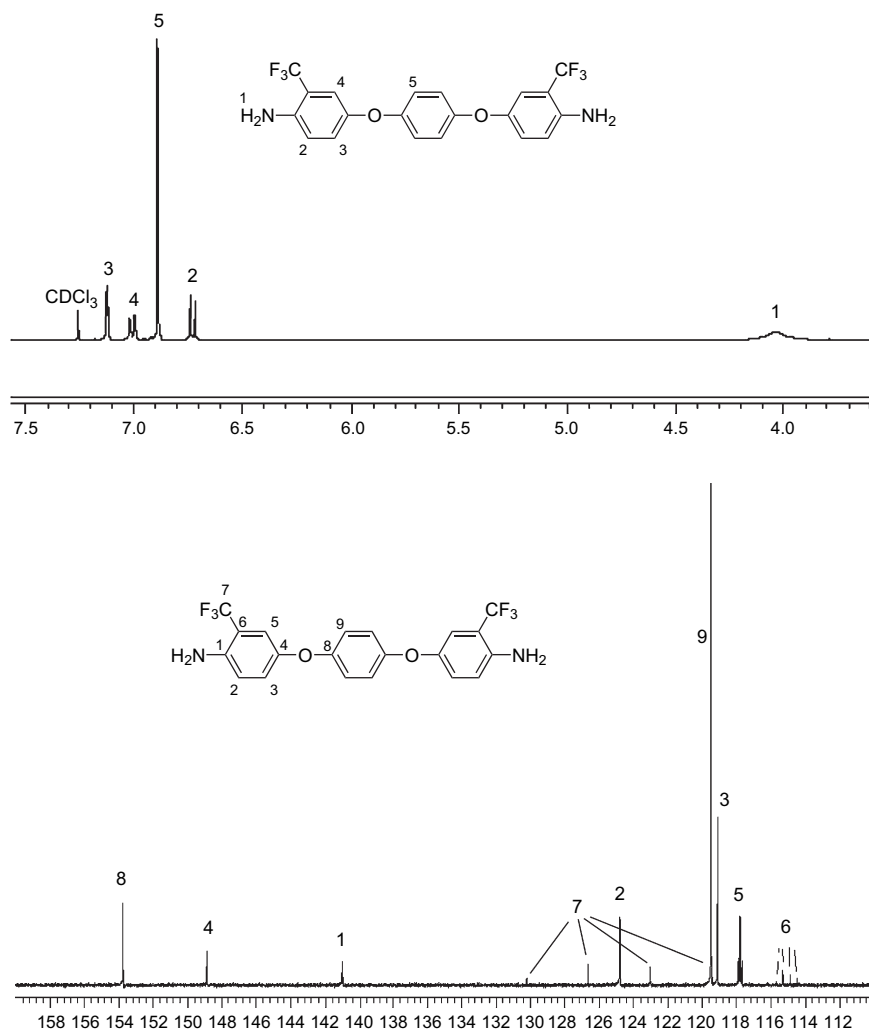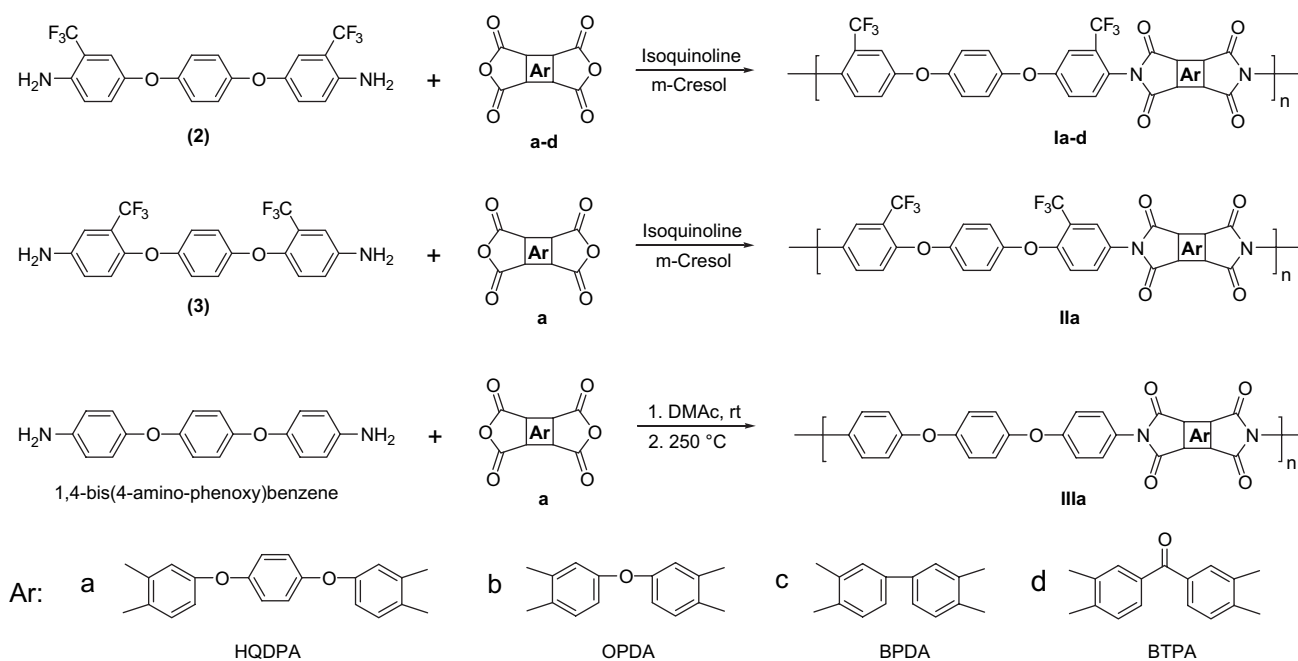
Fig. 1. FT-IR of dinitro (1) and diamine (2).

Fig. 2. ^1H and ^{13}C NMR spectra of 1,4-bis(4-amino-3-trifluoromethylphenoxy)benzene in CDCl$_3$.

Scheme 2. Synthesis of polyimides derived from diamines (**2**, **3**).

Table 1
Properties of the polyimides

Polymer	η_{inh}[a] (dl/g)	M_n[b]	M_w[b]	T_g[c] (°C)	$T_{d5\%}$[d] (°C) In N_2	In air	Char yields (%)	Transparency onset (nm)
Ia	0.70	4.5	14.2	229	532	507	57	361
Ib	0.65	3.6	7.5	241	525	496	54	363
Ic	0.97	6.1	18.7	279	533	505	55	368
Id	0.75	5.7	20.3	261	510	486	55	375
IIa	0.86	–	–	205	535	511	57	370
IIIa	–	–	–	208	540	512	53	387

[a] Inherent viscosity was measured in *N,N*-dimethylacetamide (DMAc) solution at a concentration of 0.5 dl/g at 30 ± 0.1 °C.
[b] Relative to polystyrene standards, using THF as the eluent.
[c] Glass transition temperature (T_g) measured on DSC at a heating rate of 20 °C/min.
[d] Temperature at which a 5% weight loss occurred when the polymers were placed to TGA with a heating rate of 10 °C/min.

was prepared using the two-step method. As shown in Table 1, all polyimides (**Ia–d**) had inherent viscosities in the range of 0.65–0.97 dl/g in DMAc. The weight average molecular weight of four THF soluble polyimides (**Ia–d**) were recorded in the range of $7.5–20.3 \times 10^4$ g/mol based on polystyrene standard. The molar masses were sufficiently high to form flexible and transparent films. The inherent viscosity of polyimide **Ia** is lower than that of polyimide **IIa**. This could be contributed to the lower activity of 1,4-bis(4-amino-3-trifluoromethylphenoxy)benzene (**2**) owing to the relatively larger steric hindrance of the CF$_3$ group *ortho* to the reactive amino groups compared with the CF$_3$ group *meta* to the amino group [38].

Elemental analysis and ^{1}H NMR of the polyimides were consistent with its expected structure. FT-IR spectra of these polyimide exhibited characteristic absorption bands at around 1780 and 1720 cm^{-1} due to the asymmetric and symmetric stretches of the carbonyl group of imide, and did not show an amide carbonyl peak at 1650 cm^{-1}, indicating complete imidization during polycondensation.

3.3. Polymer properties

The qualitative solubility of the polyimides is listed in Table 2. Polyimide **I** series were soluble in organic solvents,

Table 2
Solubility of polyimides

Polymer	Acetone	THF	DMF	DMSO	DMAc	NMP	CHCl$_3$
Ia	–	+	+	+	+	+	+
Ib	–	+	+	+	+	+	+
Ic	–	+	+	+	+	+	+
Id	–	+	+	+	+	+	+
IIa	–	–	+	+	+	+	–
IIIa	–	–	–	–	–	–	–

The solubility was determined at 5% solid content. +: soluble; the solid polymer was completely dissolved in the solvent to afford a clean, homogenous solution. –: insoluble; the solid polymer did not dissolve in the solvent.

such as chloroform, THF, DMSO, DMAc and NMP and could be dissolved at 5% w/v at room temperature. Polyimide **IIa** is also soluble in high boiling point solvents such as NMP, DMF, DMAc and DMSO, but not soluble in THF, and CHCl$_3$. Compared with polyimide **IIIa**, which is not soluble in common solvents, the solubility of **Ia** and **IIa** is enhanced due to the introduction of pendant CF$_3$ group. Relative to changes in structure in the diamine component, polyimide **Ia** exhibited better solubility behavior than that of comparable polyimide **IIa**. Apparently, such an improvement in solubility can be attributed to the bulky CF$_3$ substituents introduced at the *ortho*-position of nitrogen, which appears to hinder the rotation of C–N imide bond and force the two phenyl rings into adopting a noncoplanar conformation. This, in turn, disrupts the crystal packing and provides enhanced solubility. Thus, the effect of substituents in the *ortho*-positions of nitrogen on solubility was greater than the effect of substituents in the *meta*-positions.

The glass transition temperatures of polyimides are listed in Table 1. The T_g of polymer could be read in the second heating trace of DSC. The T_g of polyimide **I** series were in the range of 229–279 °C, which increased in the order of BPDA > BTPA > ODPA > HQDPA. Polyimide **Ia** obtained from HQDPA showed the lowest T_g because of the presence of two flexible ether linkages between the phthalimide units. Polyimide **Ic** exhibited the highest T_g due to the rigid biphenyl dianhydride unit. From Table 1, it can be seen that the T_g of polyimide **Ia** was higher than that of comparable polyimide **IIa**. The introduction of bulky groups into the *ortho*-position of the imide nitrogen hinders the rotation around C–N bonds of the two phenyl rings and further increases the chain rigidity is an additional evidence. The T_g value of **IIa** is lower than that of **IIIa**. This is because of the introduction of the bulky CF$_3$ side groups, which decrease intermolecular interactions, thus leading to a decreased T_g.

Thermal and thermo-oxidative stabilities of the polyimides were evaluated by TGA using 5 wt% loss values for comparison, and the results are tabulated in Table 1. The temperature at 5% weight loss ($T_{d5\%}$) of polyimide **I** series stayed within 510–533 °C in nitrogen and within 486–507 °C in air. Polyimides **Ia**, **IIa**, and **IIIa**, which all have HQDPA dianhydride moieties, showed a similar temperature loss of 5%. The result indicated the effect of the substitutions on $T_{d5\%}$ is not significant.

Fig. 3 displays the dynamic storage modulus (E'), loss modulus (E″) and tan δ as a function of temperature for the polyimide based on the same HQDPA dianhydride. Regarding the peak temperature in the tan δ curves as the T_g, the T_g values obtained by DMTA were comparable to the T_g values measured by DSC technique.

The mechanical properties of polyimide films are summarized in Table 3. Polyimide **I** series had tensile strength, elongation at break, and Young's modulus in the ranges of 137–169 MPa, 12–14%, and 1.6–2.2 GPa, respectively, indicating that they could be cast into transparent, flexible and tough films.

The cut-off wavelengths (λ_0) of polyimide films were measured using UV–visible spectroscopy. The λ_0 of polyimide **I**
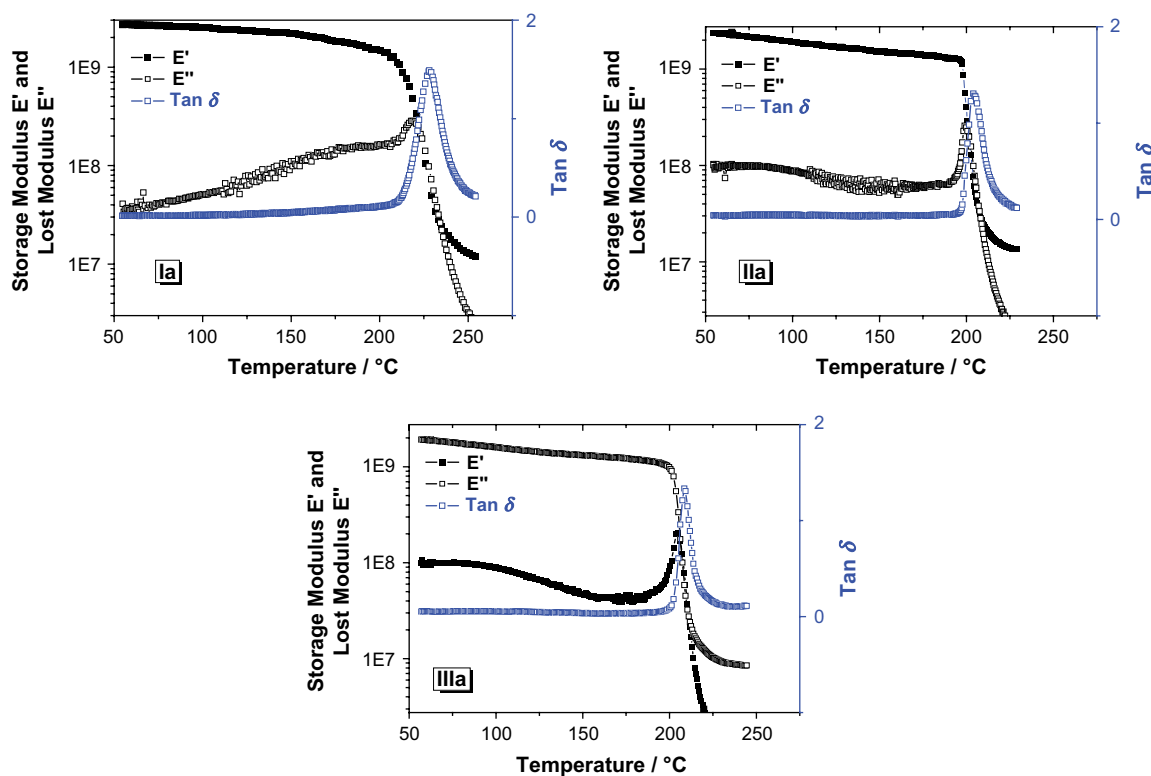
Fig. 3. Dynamic modulus as function of temperature for films of **Ia**, **IIa** and **IIIa**.

series were listed in Table 1 and ranged in 361–375 nm. The λ_0 of polyimide **I** series were affected by dianhydride moieties: the λ_0 of **Id** is the maximum, **Ib** and **Ic** revealed a shorter λ_0, and **Ia** showed the shortest λ_0. The cut-off wavelengths of **Ia**, **IIa** and **IIIa** are shown in Fig. 4 for comparison. The fluorinated polyimides **Ia** and **IIa** showed a lower cut-off wavelength and higher optical transparency than their respective CF$_3$-free analogs. This may be interpreted by reduction in the intermolecular charge-transfer complex (CTC) between alternating electron-donor (diamine) and electron-acceptor (dianhydride) moieties. Bulky and electron-withdrawing CF$_3$ group in diamine moieties was effective in decreasing the intermolecular charge-transfer complex (CTC) formation between polymer chains through steric hindrance and the inductive effect [39]. The decrease in intermolecular CTC formation is understandable also from the significant solubility of the **Ia** series polyimides with the CF$_3$ substituents. A

secondary positive effect of the CF$_3$ groups on the film transparency was the weakened intermolecular cohesive force due to the lower polarizability of the C–F bond. Polyimide **Ia** showed lower cut-off wavelengths than polyimide **IIa** due to the larger steric repulsion and inductive effect of the CF$_3$ groups on the *ortho*-position than on the *meta*-position of the imide nitrogen.

The effects of the trifluoromethyl substitution on the gas permeability of polyimides were investigated. Table 4

Table 3
Mechanical properties of polyimides films

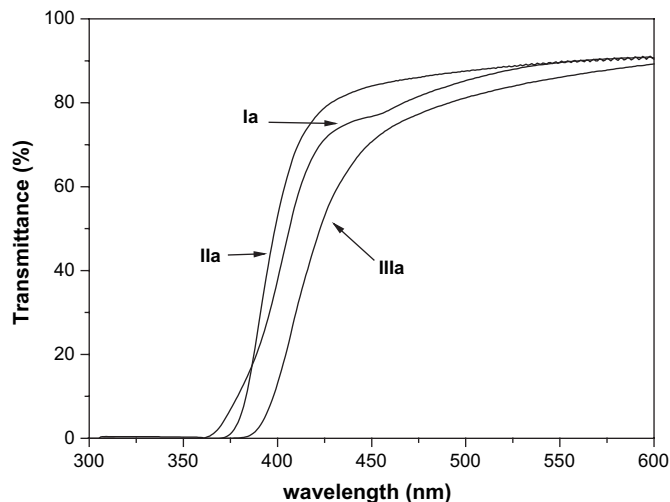| Polymers	Tensile strength (MPa)	Elongation at break (%)	Young's modulus (GPa)
Ia	137	14	1.6
Ib	143	13	1.8
Ic	169	11	2.2
Id	161	12	1.6
IIa	113	15	1.5
IIIa	93	32	2.1

Fig. 4. UV–visible spectra of **Ia**, **IIa** and **IIIa**.

Table 4
Permeability and selectivity of polyimide membranes at 1 atm and 30 °C

Membrane	Permeability (barrer)					Selectivity		
	H_2	O_2	N_2	CO_2	CH_4	H_2/N_2	O_2/N_2	CO_2/CH_4
Ia	15.28	1.378	0.2629	5.283	0.1649	58.12	5.24	32.04
Ib	18.73	1.681	0.3302	6.297	0.1981	56.72	5.09	31.79
Ic	23.44	2.075	0.4365	7.685	0.2970	53.70	4.75	25.87
Id	20.15	1.853	0.3721	7.257	0.2527	54.15	4.99	28.72
IIa	12.40	1.120	0.2113	4.468	0.1367	58.68	5.30	32.68
IIIa	5.39	0.491	0.0863	2.204	0.0628	77.48	5.69	35.10

P is permeability coefficient; units: 1 barrer $= 10^{-10} \, cm^3$ [STP] $cm \, cm^{-2} \, s^{-1} \, cmHg^{-1}$.

summarizes the result of the gas permeability and selectivity of the dense polyimide membranes for H_2, O_2, N_2, CH_4, and CO_2 measured at 30 °C and 1 atm. The permeability of O_2 and O_2/N_2 selectivity for polyimide **I** series synthesized from diamine **2** and different dianhydride were in the ranges of 1.378–2.075 barrer and 4.75–5.24, respectively. Polyimide **Ia**, **IIa**, **IIIa** based on HQDPA dianhydride showed the permeability of all tested gases in the order of **Ia** > **IIa** > **IIIa**. This can be explained by their difference in the fractional free volume (FFV). The wide angle X-ray diffraction of these polyimides is shown in Fig. 5. The curves of all the polyimides were broad and without obvious peak features, which indicate that they are all amorphous. The most prominent WAXD peak in the amorphous glassy polymer spectra is often used to estimate the average interchain spacing distance (d-spacing). The calculated d-spacing using the Bragg's equation is listed in Table 5. It is worthy to note that polyimide **Ia** displayed relatively higher fractional free volume compared with polyimide **IIa**, even though both the polyimides have the same chemical composition. Again, this can be contributed to the effect of the trifluoromethyl substitution. In comparison with **IIa**, polyimide **Ia** displayed enhanced O_2 permeability coefficient, increases from 1.120 to 1.370 barrer (22.3%), and the CO_2 permeability coefficient, from 4.468 to 5.283 barrer (18.2%). However, the O_2/N_2 permselectivity of **Ia** membrane (5.24) is comparable with that of **IIa** membrane (5.30). The results indicate that the introduction of the CF_3 groups into the *ortho*-position of the imide nitrogen is highly effective in the improvement of gas permeability while retaining the gas permselectivity.
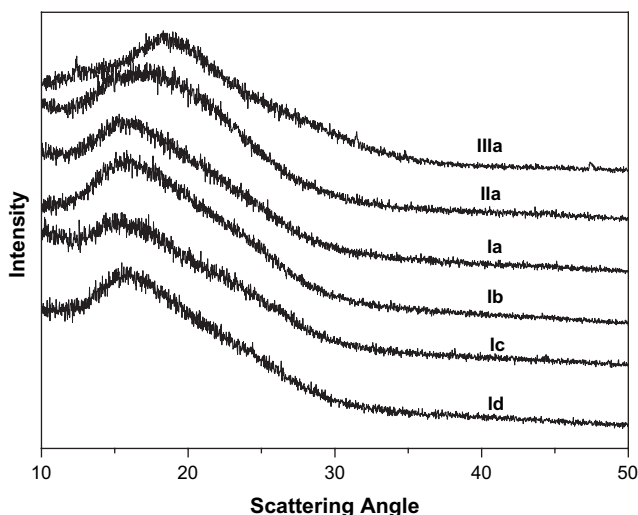
4. Conclusions

The isomeric ditrifluoromethyl substituted aromatic diamine, 1,4-bis(4-amino-3-trifluoromethylphenoxy)benzene (**2**), and a known analog 1,4-bis(4-amino-2-trifluoromethylphenoxy)benzene (**3**) were synthesized. Polyimides based on the diamine **2** exhibited better solubility, lower cut-off wavelengths (λ_0), higher T_g, and better gas permeability and permselectivity compared with polyimide **IIa** based on the diamine **3**. Such improvement in the properties could be attributed to the introduction of the bulky trifluoromethyl groups into the *ortho*-position of the imide nitrogen, which hinders the rotation of C–N imide bond and forces the two phenyl rings into a noncoplanar conformation. This, in turn, increases the free volume of polymer and retains the chain rigidity.

Fig. 5. The WAXD diagram of polyimides.

Table 5
FFV and d-spacing of the modified polyimides

Polymer	ρ (g cm^{-3})	V_{sp} (cm^{-3} g^{-1})	V_w (cm^{-3} mol^{-1})	V_0 (cm^{-3} g^{-1})	V_f (cm^{-3} g^{-1})	FFV	d-spacing
Ia	1.4598	0.685	358.28	0.586	0.099	0.145	5.50
Ib	1.4728	0.679	311.76	0.577	0.102	0.150	5.53
Ic	1.4534	0.688	306.96	0.581	0.107	0.156	5.68
Id	1.4598	0.685	318.66	0.580	0.105	0.153	5.67
IIa	1.4641	0.683	358.28	0.586	0.097	0.142	5.12
IIIa	1.3831	0.723	320.66	0.633	0.090	0.124	4.82

Acknowledgements

References

[1] Wilson D, Stenzenberger HD, Hergenrother PM, editors. Polyimides. New York: Chapman and Hall; 1990.

[2] Ghosh MK, Mittal KL, editors. Polyimides fundamentals and applications. New York: Marcel Decker; 1996.

[3] Walsh CJ, Mandal BK. Chem Mater 2001;13:2472.

[4] Al-Masri M, Fritsch D, Kricheldorf HR. Macromolecules 2000;33:7127.

[5] Mi QD, Gao LX, Ding MX. Macromolecules 1996;29:5758.

[6] Trofimenko S, Auman BC. Macromolecules 1994;27:1136.

[7] Hergenrother PM, Havens SJ. Macromolecules 1994;27:4659.

[8] Zheng HB, Wang ZY. Macromolecules 2000;33:4310.

[9] Hergenrother PM, Watson KA, Smith Jr JG, Connell JW, Yokota R. Polymer 2002;43:5077.

[10] Yan JL, Wang Z, Gao LX, Ding MX. Polymer 2005;46:7678.

[11] Yi MH, Huang W, Jin MY, Choi KY. Macromolecules 1997;30:5606.

[12] Spiliopoulos IK, Mikroyannidis JA, Tsivgoulis GM. Macromolecules 1998;31:522.

[13] Mikroyannidis JA, Tsivgoulis GM. J Polym Sci Part A Polym Chem 1999;37:3646.

[14] Spiliopoulos IK, Mikroyannidis JA. Polymer 1996;37:3331.

[15] Yoshida S, Hay AS. Macromolecules 1997;30:5979.

[16] Liu YL, Hsu CY, Wu CS. J Appl Polym Sci 2003;89:791.

[17] Spiliopoulos IK, Mikroyannidis JA. Macromolecules 1996;29:5313.

[18] Spiliopoulos IK, Mikroyannidis JA. Polymer 1997;38:2733.

[19] Chung IS, Park CE, Ree M, Kim SY. Chem Mater 2001;13:2801.

[20] Kulkarni M, Kothawade S, Arabale G, Wagh D, Vijayamohanan K, Kulkarni RA, et al. Polymer 2005;46:3669.

[21] Qiu ZM, Zhang SB. Polymer 2005;46:1693.

[22] Kim HS, Kim YH, Ahn SK, Kwon SK. Macromolecules 2003;36:2327.

[23] Hua ZQ, Wanga MH, Lia SJ, Liua XY, Wu JH. Polymer 2005;46:5278.

[24] Liaw DJ, Chang FC, Leung MK, Chou MY, Muellen K. Macromolecules 2005;38:4024.

[25] Yang CP, Su YY. Polymer 2005;46:5778.

[26] Yin DX, Li YF, Yang HX, Yang SY, Fan L, Liu JG. Polymer 2005;46:3119.

[27] Banerjee S, Madhra MK, Salunke AK, Jaiswal DK. Polymer 2003;44:613.

[28] Liaw DJ, Chang FC. J Polym Sci Part A Polym Chem 2004;42:5766.

[29] Chung CL, Yang CP, Hsiao SH. J Polym Sci Part A Polym Chem 2006;44:3092.

[30] Xie K, Zhang SY, Liu JG, He MH, Yang SY. J Polym Sci Part A Polym Chem 2001;39:2581.

[31] Suzuki T, Yamada Y, Tsujita Y. Polymer 2004;45:7167.

[32] Chuang KC, Kinder JD, Hull DL, McConville DB, Youngs WJ. Macromolecules 1997;30:7183.

[33] Lin SH, Li F, Cheng SZD, Harris FW. Macromolecules 1998;31:2080.

[34] Li YS, Ding MX, Xu JP. Polymer 1996;37:3451.

[35] Lin WH, Vora RH, Chung TS. J Polym Sci Part B Polym Phys 2000;38:2703.

[36] Wereta A, Gehatia MT. Polym Eng Sci 1979;18:204.

[37] Bondi A. J Phys Chem 1964;68:441.

[38] Hougham G, Tesoro G, Shawt J. Macromolecules 1994;27:3642.

[39] Ando S, Matsuura T, Sasaki S. Polym J 1997;29:69.